Front. Optoelectron. China 2008, 1(3–4): 201–204
DOI 10.1007/s12200-008-0041-1

RESEARCH ARTICLE

Applications of scanning femtosecond laser-induced ionization microscopy in biological imaging

Youbo ZHAO, Yanmei LIANG, Xiaonong ZHU (✉)

Institute of Modern Optics, Nankai University, Key Laboratory of Opto-electronic Information Science and Technology, Ministry of Education of China, Tianjin 300071, China

Abstract The applicability and potential advantages of femtosecond laser-induced ionization microscopy in examining biological samples are demonstrated. High-resolution section images of the inner structures and the topographical surface profiles of a piece of unstained onion skin and a human oral epithelium specimen are obtained by collecting the plasma emission signals generated either inside the samples or from air in the vicinity. It is concluded that the high material discrimination capability and the minimum damage effect give this laser-induced ionization imaging technique great potentials in the area of biological imaging and medical analyses.

Keywords nonlinear microscopy, laser-tissue interaction, ultrafast laser, bio-imaging

1 Introduction

Optical microscopes have become ubiquitous tools in medical diagnoses and biological analyses. To improve the image contrast of transparent biological specimen, sample labeling, staining and fluorescing techniques are often employed [1,2]. With the help of compact and reliable femtosecond laser sources, several types of nonlinear microscopes, such as the second- or the third-harmonic generation microscopes and the coherent anti-Stokes Raman scattering microscope, have also been developed [3–5]. These new types of microscopes have desirable advantages such as a higher spatial resolution, the capability for two- or three-dimensional imaging, and a process without staining the samples in characterizing biological specimen.

Recently, it has been reported that a novel nonlinear imaging method of laser-induced ionization microscopy is capable of mapping out subtle variations of elemental and/or structural properties of the sample materials. This new imaging technique is based on the principle that the plasma emission associated with the atomic or molecular ionization by the femtosecond laser pulses contains information on both chemical and physical properties of the sample in its ionized area. It is thus called laser-induced air ionization microscopy (LIAIM) [6] or laser-induced breakdown microscopy (LIBM) [7], depending on the location of the ionization, which is either in the air or directly inside the sample. It has been demonstrated that either LIAIM or LIBM has the combined advantages of nonlinear scanning optical microscopes and laser-induced breakdown spectroscopy (LIBS) [8–12]. In this paper, the applicability of this technique of femtosecond laser-induced ionization microscopy is exploited in examining biological samples. The LIAIM and LIBM images of some non-elaborately chosen biological specimens, such as onion skin cells and human oral epithelium cells, are presented. The potential applications of this technique in both medical imaging and biological studies are confirmed.

Received September 19, 2007; accepted November 22, 2007

E-mail: xnzhu1@nankai.edu.cn

2 Experiments

The schematic diagram of the experimental set-up is shown in Fig. 1. The femtosecond laser system (Spectra Phys. Inc. HP-Spitfire) employed in our experiments for plasma generation has an output of 1 kHz, 50 fs pulses and a central wavelength of around 800 nm. While the maximum pulse energy of this laser system can reach approximately 2 mJ, the typical pulse energy of a few tens of nano Joules is sufficient for the imaging experiments. The attenuation of the laser power is achieved through a programmable half-wave plate/polarizer-based attenuator together with some neutral density filters. The linearly polarized laser beam, after being reflected by two 45° steering mirrors (M1, M2), is focused on the sample at normal incidence by a 10× microscopic objective. The

plasma emission signal is collected through the same objective in the backward direction and detected by a photomultiplier (PMT) (Hamamatsu, 212UH). A dichroic mirror, M2, with an reflection >95% for a 750–850 nm wavelength range, and a short-pass optical filter with a cut-off wavelength of 700 nm are inserted before the PMT in the beam path. The photoelectric signal from the PMT is amplified by a lock-in amplifier (Stanford Research Systems, SR830), and the amplified signal is then fed into the computer via a data acquisition card. The sample of interest, mounted on an assembly of three motorized translation stages (all from Newport, UTM 100 PPE.1), is translated point by point in the plane normal to the laser beam during the process of imaging acquisition.

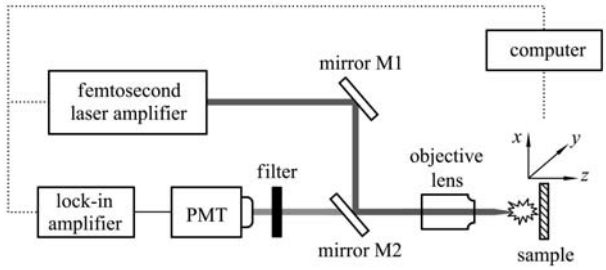

Fig. 1 Schematic diagram of experimental set-up

3 Results and discussion

Shown in Fig. 2(a) is the LIBM image of a segment of the outer skin from a fresh onion, which is pasted on a microscopic slide, and the imaging process begins approximately two hours after the sample's preparation. To obtain this image, the sample is scanned with a scanning step of 3 μm by a 10× objective (numerical aperture, NA, is 0.25). At each step, the sample is maintained at rest for approximately 300 ms, and it takes about 4 hours to obtain the entire image. For comparison, the image of the same area of the onion skin obtained with an ordinary microscope (Olympus BX51) is reproduced in Fig. 2(b). Figures 2(c) and 2(d) present the pseudo-color transformed versions of Figs. 2(a) and 2(b), respectively. By comparing these images, it can be seen that the main cell structures are resolved in the LIBM image. Moreover, the cell walls and the nuclei in Figs. 2(a) and 2(c) are apparently sharper than those in Figs. 2(b) and 2(d), which indicates the improved depth resolution and inherent optical sectioning capability of LIBM. Such advantages may be attributed to the nonlinear nature of this laser-induced ionization probe. In nonlinear detection, the detected signal only comes from the very proximity of the laser focus, and the background light out of the focus area is significantly depressed. In the ordinary micrographs shown by Figs. 2(b) and 2(d), however, more detailed structures can be observed, which can be regarded as the result of a better lateral resolution associated with the use of a higher NA objective. The information of out-of-focus structures is also presented. In fact, it is only this latter feature that sets the limitations of conventional microscopes in obtaining depth information, especially for transparent and relatively thick samples.

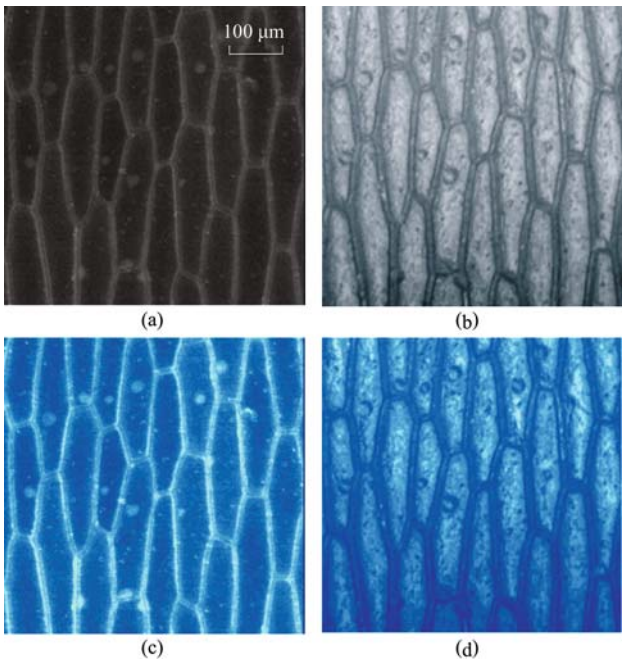

Fig. 2 Microscopic images of a segment of onion skin. (a) LIBM image taken by a 10× objective with a scanning step of 3 μm; (b) micrograph of the same sample area taken by an ordinary optical microscope (Olympus BX51, 200× magnification) with differential interference contrast function; (c) pseudo-color image of (a); (d) pseudo-color image of (b)

Apparently, the spatial resolution in LIBM can be improved if an objective with higher NA is used. The same area of the onion sample scanned by a 40× objective (NA = 0.65) with a scanning step of 1 μm is shown in Fig. 3. In this picture, the cell wall and the nucleus can be clearly discriminated. A few bright spots are also observed inside the cells, which are likely to be the mitochondria or other organelles. It is noted that the stronger ionization emission signal is normally generated from the organelles, such as the nucleus and nucleoli. The laser-induced ionization or breakdown of the various protein molecules within organelles is probably the primary origin of the measured plasma emission signals.

The three-dimensional images of the examples obtained by using LIBM through layer-by-layer scanning are illustrated in Fig. 4, where images of consecutive scans are shown at four different depth levels. Figure 4(a) is the LIBM image of the top layer of the cells, while Figs. 4(b) to 4(d) present images for deeper layers. The separation between any two neighboring layers is approximately 5 μm, and the distance from the top layer to the sample

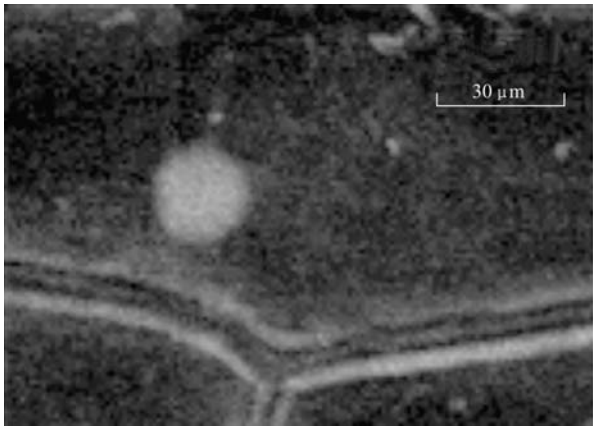

Fig. 3 LIBM image of a segment of a piece of onion skin

surface is approximately 20 μm. Within the given field of view of these four images, a segment of the plasmolyzed cell in the dried onion skin is revealed. From these images, some subtle differences can be found in the micro structures of the exposed onion cells at different layers. It is interesting to note that in Figs 4(b) and 4(c), some fine structures in the nucleus are actually visible. For example, two nucleoli of the cells are seen to be oriented along the 45° direction.

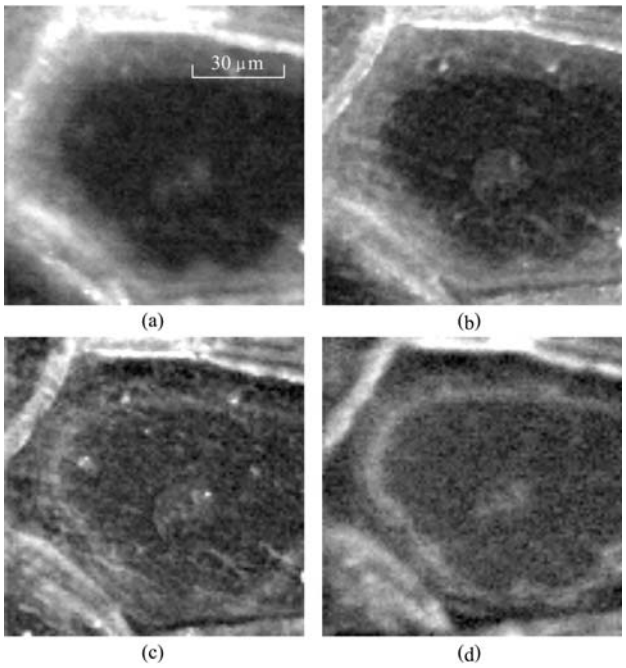

Fig. 4 LIBM images taken by a 40× objective with a scanning step of 1 μm in four different layers of an onion skin

It is also worth mentioning that when these LIBM images are obtained, the scanning plane is actually inside the cells. This means that the collected plasma signal is generated from direct ionization of the substance of the cell, thus making the image contrast between different areas of the cells reflect the variation of the biological structure and (or) substance. This high resolution power, used to distinguish elemental composition and (or) physical structure of the sample, is critical for the applications in medical diagnoses such as identifying pathological changes from normal tissues, which has been exploited by LIBS [10] but not in an imaging mode.

In Fig. 5(a), a LIBM image of a cell of human oral epithelium is shown. This image is obtained by using the 40× objective with a scanning step of 1 μm. As clearly shown in this image, a round nucleus is at the center of the cell. Since the scanning plane is inside the cell, this image can in fact reveal the inner structure of the cell. As already mentioned above, another version of laser-induced ionization microscopy is adopted to image the surface profile of the sample of interest by using the sample surface-assisted air ionization probe known as LIAIM [6]. In such a case, focus of the excitation beam is carefully located directly above the sample surface so that air in the vicinity can be ionized with the initial photoelectron seeds from the surface. With this approach, the collected air plasma emission signal will be sensitive to properties of the elemental composition or topography of the sample surface. The LIAIM image of the surface profile of the same cell shown in Fig. 5(a) is reproduced in Fig. 5(b). In this situation, since changes of the material properties are likely to be minimal on the cell surface, the LIAIM image actually presents the depth-resolved topographical profile of the surface. It is worth mentioning that the bright spot related to increased signal strength, near the center of this image, is in fact due to the bulge of the nucleus. The two images of

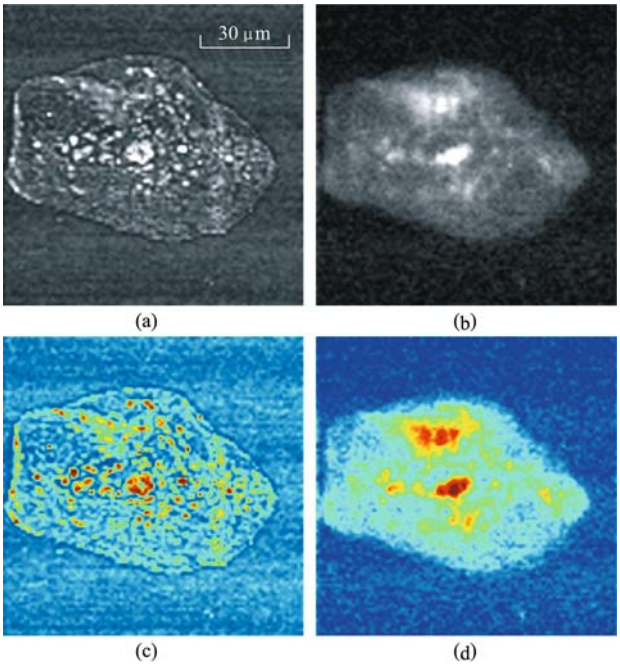

Fig. 5 Images of a human oral epithelium cell. (a) LIBM image; (b) LIAIM image; (c) pseudo-color image of (a); (d) pseudo-color image of (b)

Figs. 5(a) and 5(b) clearly demonstrate that the ionization-related nonlinear microscopic images of either embedded microstructures or surface profiles of the transparent biological samples can be obtained by setting the laser focal point at desired positions. Some commonly used imaging processing techniques can be also adopted to further improve the quality of LIBM or LIAIM images. For examples, Figs. 5(c) and 5(d) show the pseudo-color enhanced images of Figs. 5(a) and 5(b) respectively.

For nonlinear imaging of any biological specimen, it is important to minimize or avoid any kind of laser-induced damage to the samples. In our experiments, a highly sensitive PMT is used to detect the compound plasma emission in the visible spectral range, so that a good signal-to-noise ratio (SNR) could be achieved without raising excitation intensity. In our set-up, the effective laser intensity at the focus is estimated to be approximately 3×10^{12} W/cm^2, which is normally lower than the damage threshold of the biologic tissues [13,14]. To ensure that no severe optical damage occurs, the same sample area is normally scanned several times and steps are taken to find out if any difference in imaging quality from different scans exists. A good consistency among different scans is observed, which implies that damage to the samples is negligible. In LIAIM, since ionization takes place in the surrounding air, the possibility of laser-induced damage on the samples can be further minimized by properly choosing the laser parameters and distance between the laser focal point and the sample surface.

4 Conclusions

In summary, the applicability and huge potential of femtosecond laser-induced ionization microcopy have been demonstrated in imaging biological samples. Given its inherent nonlinear nature and high sensitivity to both chemical and physical properties of samples under testing, the femtosecond laser-induced ionization probe can provide sectioning images of the unstained transparent biological specimens with high resolution. Through proper adjustment of the intensity and focal position of the femtosecond laser beam, nonlinear mapping of either the inner microstructure or surface profile of a transparent biologic sample can be achieved. The three-dimensional images through layered scanning can be also obtained by this technique without requiring a confocal set-up. Although lateral resolutions of the presented LIBM and LIAIM images are still at the micron level, it is believed that nanometer-level resolution could be achieved in the future by using objectives with large numerical aperture and raising the position resolution of the translation stages. The high material discrimination power and minimal damage to the samples under examination also make this method attractive in pathological diagnoses. It is believed that this technique can be further developed into an *in vivo* method and combine the functions of imaging and therapy by properly adjusting the system parameters.

Acknowledgements This project was supported by the State Key Program of National Natural Science Foundation of China (Grant No. 60637020). The authors would like to thank Wang M and Yang J for their technical assistance.

References

1. Török P, Kao F J. Optical Imaging and Microscopy. Berlin: Springer-Verlag, 2003
2. Denk W, Strickler J H, Webb W W. Two-photon laser scanning fluorescence microscopy. Science, 1990, 248(4951): 73–76
3. Boulesteix T, Beaurepaire E, Sauviat M P, et al. Second-harmonic microscopy of unstained living cardiac myocytes: measurements of sarcomere length with 20-nm accuracy. Optics Letters, 2004, 29(17): 2031–2033
4. Squier J, Muller M, Brakenhoff G, et al. Third harmonic generation microscopy. Optics Express, 1998, 3(9): 315–324
5. Cheng J X, Volkmer A, Book L D, et al. An epi-detected coherent anti-Stokes Raman scattering (E-CARS) microscope with high spectral resolution and high sensitivity. Journal of Physical Chemistry B, 2001, 105(7): 1277–1280
6. Zhao Y, Zhang N, Yang J, et al. Laser-induced air ionization microscopy. Applied Physics Letters, 2006, 88(24): 241102
7. Zhao Y, Mu G, Zhu X. Nonlinear imaging of embedded microstructures inside transparent materials with laser-induced ionization microscopy. Optics Letters, 2006, 31(18): 2765–2767
8. Cremers D A, Radziemski L J. Handbook of Laser-induced Breakdown Spectroscopy. London: John Wiley & Sons, 2006
9. Tognoni E, Palleschi V, Corsi M, et al. Quantitative micro-analysis by laser-induced breakdown spectroscopy–a review of the experimental approaches. Spectrochimica Acta Part B, 2002: 57(7): 1115–1130
10. Kumar A, Yueh F Y, Singh J P, et al. Characterization of malignant tissue cells by laser-induced breakdown spectroscopy. Applied Optics, 2004, 43(28): 5399–5403
11. Samek O, Telle H H, Beddows D C. Laser-induced breakdown spectroscopy: a tool for real-time, in vitro and in vivo identification of carious teeth. BMC Oral Health, 2001, 1(1): 1–9
12. Menut D, Fichet P, Lacour J L, et al. Micro-laser-induced breakdown spectroscopy technique: a powerful method for performing quantitative surface mapping on conductive and nonconductive samples. Applied Optics, 2003, 42(30): 6063–6071
13. Birngruber R, Puliafito C A, Gawande A, et al. Femtosecond laser-tissue interactions: retinal injury studies. IEEE Journal of Quantum Electronics, 1987, 23(10): 1836–1844
14. Loesel F H, Fischer J P, Götz M H, et al. Non-thermal ablation of neural tissue with femtosecond laser pulses. Applied Physics B, 1998, 66(1): 121–128